STABILITY OF CHEMICAL REACTION IN FLUID CATALYTIC REACTORS

SHINTARO FURUSAKI, MICHIO TAKAHASHI
AND TERUKATSU MIYAUCHI
Department of Chemical Engineering,
University of Tokyo, Tokyo 113

Effect of the freeboard and the transition region on stability of fluid catalytic reactors is presented. Wall heat transfer coefficient and solid circulation rate have a significant effect on stability. These properties were measured. Both decrease as bed density decreases in the dilute phase (freeboard) and transition region. On the premise that non-catalytic violent reactions are induced due to temperature rise initiated by catalytic reactions in the dilute phase and/or the transition region, an approach to instability of the reaction system is presented by calculations. If the non-catalytic reactions are highly exothermic and their activation energies are large, the system can easily run away at any level of solid circulation. Thus, the possibility of these non-catalytic reactions, e. g. combustion or polymerization, should be avoided by such means as control of inlet compositions or close control of temperature in the dilute phase.

Introduction

Fluid catalytic reactors are widely applied to reactions with large heat of reaction because of their good thermal transportation throughout the bed. Axial distribution of contact efficiency in the reactor is sometimes important in considering selectivity and stability. This distribution was studied experimentally[9] and it was found that the freeboard (dilute phase) and the transition region to the freeboard were very efficient in solid-gas contact, as well as the region just above the distributor. Selectivity in several reaction schemes was studied as the effect of the distribution, and the effect of the freeboard was found significant, especially for the case of highly exothermic reactions[16].

Stability as well as selectivity is important in the operation of fluid bed reactors[3,5]. Actually uncontrollable reactions are reported for naphthalene oxidation[17] and catalytic cracking[24]. It is widely known that precaution against afterburning is necessary in designing fluid catalytic reactors. In discussing stability inside reactors, several factors of stability are to be considered[6,8,18], i. e. multiplicity of steady states, local stability against perturbation, sensitivity to external conditions and oscillation. In the case of fluid catalytic reactors, characteristic features arise from the existence of moving particles. The purpose of this paper is to describe the significance of the dilute phase[25] in considering instability of fluid catalytic reactors. The concept of successive contact[14] is applied to analysis.

Received November 30, 1977. Correspondence concerning this article should be addressed to S. Furusaki. M. Takahashi is with Kureha Chemical Industries, Ltd., Iwaki-shi 974.

1. Factors Affecting Stability in Fluid Catalytic Reactors

Stability in fluid beds is somewhat different in aspect from that in fixed-bed reactors. Sensitivity in fixed-bed reactors was discussed by Froment[8] and Endoh *et al.*[6]. They showed that multiple steady states and oscillation were rare since longitudinal mixing of gas phase was small and solid particles were fixed in their positions. In the case of fluid-bed reactors, longitudinal mixing of solid particles is much larger in magnitude. Flow of gas phase is rather complicated due to the existence of bubbles, but it is probable that thermal feedback predominates over feedback of the reactant. Thus, there is a possibility of multiple steady states. On the other hand, stability against perturbation increases due to solid mixing. However, it decreases in the freeboard because of the smaller heat transfer rate. This may induce runaway phenomena in the dilute phase. Thus the dilute phase plays important roles in the stability of fluid catalytic reactors. The schematic features of the fluid catalytic reactor are described elsewhere[14,16] and are sketched in **Fig. 1**.

Reactions in the dilute phase are generally calculated by the following equations by the use of a one-dimensional homogeneous model.

$$E_f\frac{\partial^2 c}{\partial z^2}-U_f\frac{\partial c}{\partial z}-\eta_c\left(\frac{\rho_b}{\rho_{de}}\right)\varepsilon_{ede}R_c(c,T)-R_{nc}(c,T)=\frac{\partial c}{\partial t} \quad (1)$$

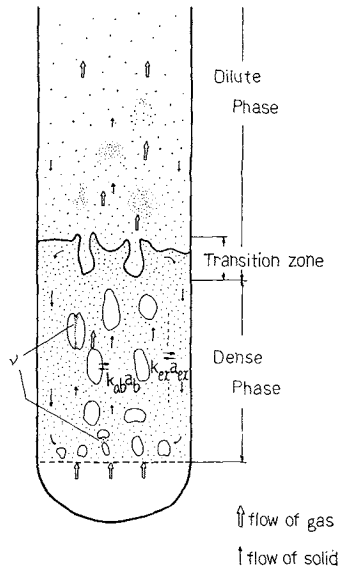

Fig. 1 Reactor model of a fluid bed

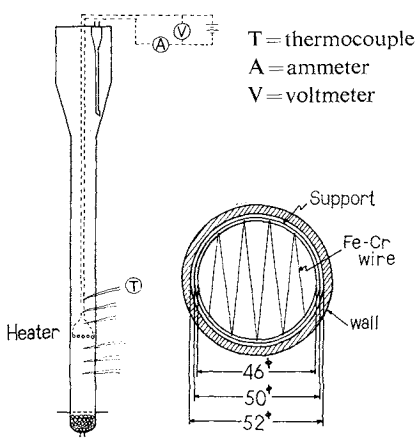

(a) Test apparatus (b) Detail of the heater

Fig. 2 Measurement of solid circulation

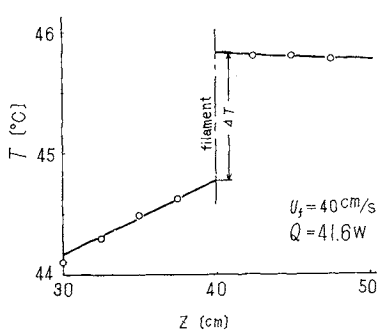

Fig. 3 Jump of temperature at the level of the heater

$$k_H\frac{\partial^2 T}{\partial z^2}-U_f c_{pf}\rho_f\frac{\partial T}{\partial z}-\eta_c\left(\frac{\rho_b}{\rho_{de}}\right)(\Delta H)_c\varepsilon_{ede}R_c(c,T)$$
$$-(\Delta H)_{nc}R_{nc}(c,T)-h_w a_w(T-T_c)=c_{pb}\rho_b\frac{\partial T}{\partial t} \quad (2)$$

These equations reveal several factors affecting stability in the dilute phase, i.e., E_f, k_H, h_w. Data on these properties are rare in the literature. In this paper, $E_f=0$ is assumed. The longitudinal mixing of solid particles and wall heat transfer coefficient are important in considering stability, and they were measured before performing the calculations.

2. Axial Mixing of Solid Particles

Solid particles are seemingly circulated as in the dense phase, ascending in the central core and descending along the periphery. The circulating flow was measured as described in the following section.

2. 1 Experimental apparatus

A schematic diagram of the measuring device is shown in **Fig. 2**. The fluid bed was 5 cm in diameter and 120 cm in height. Heating medium of iron-chromium wire (100 μm in diameter) was put across the section of the bed to heat the ascending gas and solid flow. Temperature jump at the level of the heater was measured. To prevent the loss of heat from the bed, a thermal insulator of glass-wool was put around the bed. Direct current was conducted through the wire so that the supplied energy could be calculated. An example of the temperature increase is shown in **Fig. 3**. Circulating velocity of solid particles can be obtained from these two values, i. e. the supplied energy and the temperature jump. Heat loss from the wall was found to be negligible because the increase of gas temperature at the level of the heater balanced the supplied heat for the case of a vacant bed. Assumptions to calculate the amount of circulation are as follows. (1) The ascending and descending flows are in piston flow. (2) Heat transfer rate between gas and solid is so large that the homogeneous model may be applied. (3) Heat capacity of gas can be neglected compared with that of solid particles. (4) Half of the solid flows upward and the other half flows downward.

Taking the enthalpy balance for the ascending two-phase flow, the increase of temperature is given by the following equation.

$$-U_S A_T c_{ps}\rho_s\Delta T+Q/2=0 \quad (3)$$

From this, the circulating rate is obtained.

$$U_S=Q/2A_T c_{ps}\rho_s\Delta T \quad (4)$$

2. 2 Results

U_s thus obtained is shown in **Fig. 4** by its ratios to U_f for the case of a static bed height of 22 cm. The rate of solid circulation increases along with increase of the superficial velocity of gas flow. The effect of gas velocity is quite large, especially for the range of 10–20 cm/s. This is because the amount of entrained solid increases remarkably in this superficial velocity range. Above 20 cm/s, the value of $\lambda(\equiv U_s/U_f)$ in-

creases moderately with increase of U_f. λ decreases at higher levels in the bed since solid concentration decreases with increase of vertical position. The transition region between the dense and dilute phases is at about $z=25$ cm. The value of λ in the dense phase was uncertain because the temperature jump at the level of the heater was very small.

Since λ is a strong function of bed density, it is replotted against ρ_b/ρ_{de} in **Fig. 5**. It is obvious that λ is very small for small ρ_b. However, the effect of solid circulation on temperature distribution cannot be ignored since the heat capacity of the solid particles is several hundred times as large as that of the gas.

3. Wall Heat Transfer Coefficient[22]

Heat transfer coefficient between wall and the dense phase has been well investigated[1,10,19,26]. Also, data on heat transfer in solid-gas transport lines may be found in the literature[2,7]. However, few investigations of heat transfer between wall and dilute phase (freeboard) have been made so far. Mickley and Trilling[13] reported that h_w decreased proportionally to $\rho_b^{0.48}$. Shirai[20,21] investigated the longitudinal distribution of heat transfer coefficient by use of a spherical probe.

3. 1 Experimental procedures

Heat transfer coefficients in the dilute phase were measured by a method similar to that of Shirai *et al.*[21]. A bullet-shaped probe 0.8 cm in diameter and 4 cm in length with a heater set inside was traversed along the center of the bed. Direct current was applied to the heater. From the electric power used and the temperature difference between the surface of the probe and the emulsion phase, the heat transfer coefficient at the surface of the probe was calculated.

The packet proposed by Mickley and Fairbanks[12] was examined experimentally by Selzer and Thomson[19]. Contact time was 0.1–0.3 s and the penetration depth of heat transfer was 100–500 μm. Considering these data, the size of the probe was probably much larger than the size of the packet contacting the heating wall of the probe. Thus, data by means of this probe may be considered to represent heat transfer coefficients for vertical tube walls if the flow pattern of the emulsion is not affected by the tip of the probe. The heat transfer coefficient at the stagnant point (tip) will be different from that along the wall, but the effect is small since the wall surface area is much larger than the stagnant surface area.

3. 2 Results

Wall heat transfer coefficients thus measured are plotted in **Fig. 6**. To compare with heat transfer coefficient for the immersed vertical tubes, calculation using the correlation by Wender and Cooper[23] was carried out as shown in the figure. The experimental data for the dense phase matched the calculated values. This seems to represent the adequacy of such procedure to measure heat transfer coefficients.

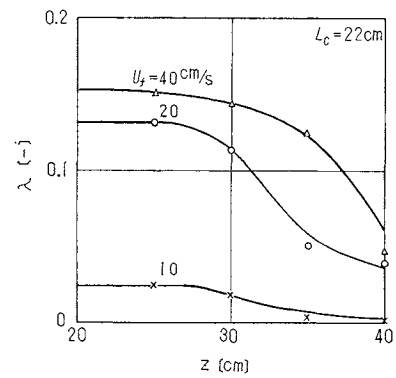

Fig. 4 Axial distribution of λ

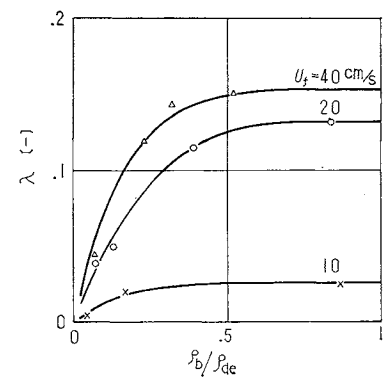

Fig. 5 Dependence of λ on the bed density

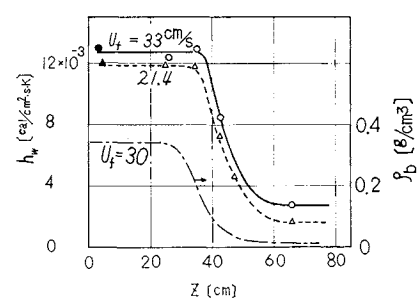

Dark points are calculated by the Wender-Cooper correlation. $L_c=30$ cm.

Fig. 6 Axial profile of wall heat transfer coefficient

Figure 6 shows that the heat transfer coefficient decreases with decrease of bed density. This is in accord with the data of Shirai[20,21]. In the transition region at about 30 cm height above the distributor, h_w is still large, having about the same value as that in the dense phase. h_w begins to decrease at the point of $\varepsilon_e \approx 0.5$. The dependence of h_w on bed density ρ_b was examined. h_w decreased proportionally to $\rho_b^{0.5}$ for the most of the dilute phase. In the upper region of the dilute phase, h_w is rather proportional to ρ_b. However, more data are necessary to investigate the general behavior of heat transfer in the dilute phase.

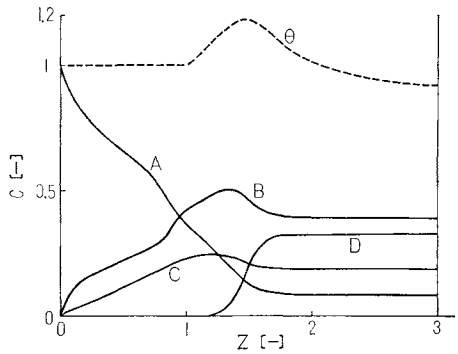

$N_{r1}=2\times10^{8}$, $N_{r2}=N_{r1}/10$, $N_{r3}=1.08\times10^{13}$,
$E_1=E_2=83.6$ kJ/mol, $E_3=167$ kJ/mol,
$N_{Pe}=0.1$, $N_{Hw}=50$, $\theta_c=0.9$, $T_{de}=573$K,
$\Omega_1=\Omega_2=1$, $\Omega_3=50$

Fig. 7 Temperature and concentration profiles

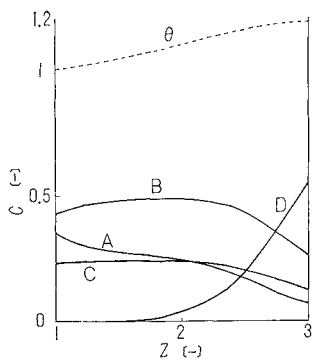

Parameters are same as Fig. 7 except $N_{Pe}=0.01$

Fig. 8 Temperature and concentration profiles for the dilute phase

4. Stability in the Dilute Phase

Based upon the results of the studies stated above, stability in the dilute phase is investigated. The most important stability problem in fluid beds is that of runaway phenomena in the freeboard and also in the space just below baffle plates located inside the dense bed. The good contact and small heat transfer rate as shown above are major causes of runaway. The most significant temperature rise is considered to occur by the coupling effect of medium temperature rise due to good contact in the dilute phase (including the transition region) and of non-catalytic reactions which are initiated by the temperature rise. Thus, a model reaction for considering possibility of runaway is shown as follows.

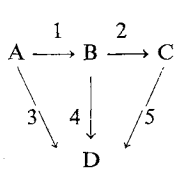

Here, A is the raw material and B is the required product. C and D are by-products, but D is produced by non-catalytic reactions, 3–5, such as combustion or polymerization. The production of D is highly exothermic and the activation energies of the reactions are large. Thus the production of D starts due to the temperature rise and this gives rise to violent reaction condition.

As the rate of solid circulation in the dilute phase is a function of solid concentration, a definite value of the extent of solid mixing is difficult to set up. Here, several values are assumed in calculation.

Steady-state profiles of temperature and concentrations of reactants are calculated since an observable approach to unstable runaway phenomena can be visualized. Material balances and enthalpy balance in the dilute phase are given by the following equations in dimensionless forms.

$$\frac{dC_A}{dZ}+\nu N_{Ar1}\,e^{-\Gamma_1/\theta}C_A+N_{Ar3}\,e^{-\Gamma_3/\theta}C_A=0 \tag{5}$$

$$\frac{dC_B}{dZ}+\nu(N_{Ar2}\,e^{-\Gamma_2/\theta}C_B-N_{Ar1}\,e^{-\Gamma_1/\theta}C_A)+N_{Ar4}\,e^{-\Gamma_4/\theta}C_B=0 \tag{6}$$

$$\frac{dC_C}{dZ}-\nu N_{Ar2}\,e^{-\Gamma_2/\theta}C_B+N_{Ar5}\,e^{-\Gamma_5/\theta}C_c=0 \tag{7}$$

$$\frac{1}{N_{Pe}}\frac{d^2\theta}{dZ^2}-\frac{d\theta}{dZ}+\nu(\Omega_1 N_{Ar1}\,e^{-\Gamma_1/\theta}C_A+\Omega_2 N_{Ar2}\,e^{-\Gamma_2/\theta}C_B)+(\Omega_3 N_{Ar3}\,e^{-\Gamma_3/\theta}C_A+\Omega_4 N_{Ar4}e^{-\Gamma_4/\theta}C_B+\Omega_5 N_{Ar5}\,e^{-\Gamma_5/\theta}C\ )-N_{Hw}(\theta-\theta_c)=0 \tag{8}$$

The boundary conditions for the above equations are, at $Z=1$, $C_A=C_{A1}$, $C_B=C_{B1}$, $C_C=C_{C1}$, $\theta=1$; and at $Z=Z_t$, $d\theta/dZ=0$. For simplicity, $N_{Ar3}=N_{Ar4}=N_{Ar5}$, $\Gamma_3=\Gamma_4=\Gamma_5$ and $\Gamma_1=\Gamma_2$ are assumed. ν is the fraction of catalyst which contacts the gas phase directly, and this value was obtained from experiments of hydrogenation of ethylene as a function of z[15]. N_{Pe} is a Peclet number accounting for the thermal diffusion due to solid mixing. If N_{Pe} is zero, temperature is completely uniform in the dilute phase. N_{Hw} is a dimensionless heat transfer coefficient and sometimes the effect of radiative transfer is to be accounted for.

Examples of concentration and temperature profiles for several values of N_{Pe} are shown in **Figs. 7** and **8**. Reaction 1 is an ordinary reaction with an activation energy of 83.6 kJ/mol (20 kcal/mol), and the rate of reaction 2 is chosen as one-tenth that of reaction 1. The non-catalytic reactions 3–5 are violent, with an activation energy of 167 kJ/mol and heat of reaction (A→D) of about 3×10^3 kJ/mol. This reaction does not occur at the temperature of the dense phase, but is quite active at higher temperatures because of the large activation energy. The value of N_{Hw}, 50, represents approximately the case for the dilute phase with effective diameter of about 5 cm. $N_{Ar1}=2\times10^8$ and $E_1=82.6$ kJ/mol mean $k_{r1}L_f/U_f=5$.

$\Omega_3=50$ means $-\Delta H_3=2800$ kJ/mol at $c_A^\circ=6.4\times10^{-7}$ mol/cm^3 (ca. 3.0%) at 573 K and 1 atm. This heat of reaction is not so large as the heat of combustion for many hydrocarbons, but is much larger than in ordinary chemical reactions. If the concentration of reactant A is much larger, a smaller heat of reaction will be enough to give the same value of Ω_3 as above.

From these figures, it is obvious that there is considerable temperature rise in the dilute phase due to non-catalytic, highly exothermic reactions. Stability of the reaction system is very sensitive to N_{Pe} and N_{Hw}. If N_{Pe} becomes larger, the temperature rise at the bottom of the dilute phase becomes enormous and reaches uncontrollable values.

The case of large N_{Pe} may be studied by calculation for the case of unmixed solid particles. Calculations of this case show that cooling of the dilute phase is necessary for operating the reactor in steady state for such unstable reactions. **(Fig. 9)**

The extreme case of small N_{Pe} is the case of the thermally complete-mixed dilute phase. It is possible for multiple steady states to exist in this case. Examples of analyses by heat generation and rejection curves, proposed by van Heerden[27], are shown in **Fig. 10**. The effect of radiation is calculated simply assuming that particle swarms of emissivity 0.8 stay near the wall. The enthalpy balance in the dilute phase in calculating these figures is described below. The material balances are calculated by assuming piston flow of the gas phase as shown in Eqs. (5)–(7).

$$Q_I=\Omega_B(C_{Bo}-C_{B1})+\Omega_C(C_{Co}-C_{C1})+\Omega_D(C_{Do}-C_{D1}) \tag{9}$$

$$Q_{II}=(1+N'_H)\theta_{di}-1-N'_H\theta_c \tag{10}$$

$$Q_I=Q_{II} \quad \text{from the enthalpy balance} \tag{11}$$

where

$$\Omega_i=(-\Delta H_i)c_A^\circ/c_{pf}\rho_f T_{de} \tag{12}$$

$$N'_H=h_w a_w(L_t-L_f)/U_f\rho_f c_{pf} \tag{13}$$

Q_I and Q_{II} are dimensionless heat being generated and rejected, respectively. θ is the dimensionless temperature, and θ_c is that for the cooling wall. The value of N'_H is 100–200 for the transition zone and 30–50 for the dilute phase. There are two stable steady states and one unstable point for E_3 of 167, 293 kJ/mol. If E_3 is reduced to 40 kJ/mol, only one stable point is possible. Thus, spontaneous ignition is possible for large values of E_3 and the existence of instability is probable for these unstable reaction systems even in the case of thermal homogeneity.

Conclusion

In applying fluid catalytic reactors, unstable phenomena in the freeboard region (or the dilute phase) should carefully be investigated. Solid circulation rate and wall heat transfer coefficient are important in considering the stability in this region. Data on these properties were measured and are presented. Based upon these data, runaway phenomenon is studied for the case of catalytic reactions accompanied by non-catalytic reactions which are the main cause of the runaway. When the non-catalytic reactions are highly exothermic and have large activation energies, the possibility of runaway is very high. Therefore, suppression of the undesired non-catalytic reaction is required by means of control of feed composition of the reactant gas or control of temperature in the dilute phase.

This problem of stability in the dilute phase in fluid catalytic reactors is very important in their application, and more study is needed along with the investigation of solid circulation and heat transfer.

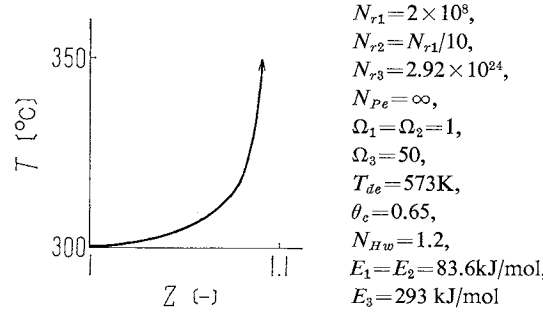

Fig. 9 Runaway for the case of no solid mixing

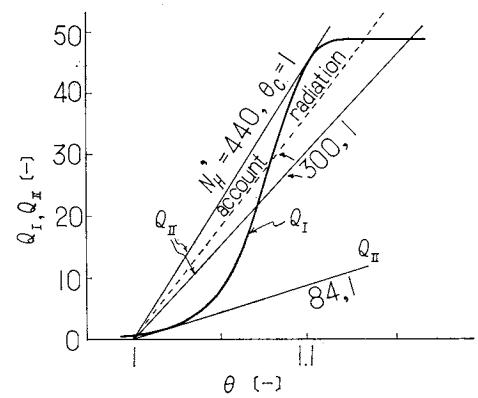

Parameters are same as Fig. 10 except that $\theta_c=1$ and $N_{pe}=0$.

Fig. 10 Multiple steady states for complete mixing of particles in the dilute phase

Acknowledgment

The authors wish to express their gratitude to Dr. S. Watarai of Tsuruoka Technical High School for useful comments on this subject.

Nomenclature

A_r	=	frequency factor in the Arrhenius expression of reaction rates	[s^{-1}]
A_T	=	cross-sectional area of the bed	[cm^2]
a_w	=	heat transfer surface area of the wall	[cm^{-1}]

C = dimensionless concentration (c/c_A°) [—]
C_{Ao}, C_{Bo} ... = dimensionless concentration of A, B, ... in the outlet gas [—]
C_{A1}, C_{B1} ... = dimensionless concentration of A, B, ... at the end of the dense phase [—]
c = concentration [mol/cm^3]
c_A° = concentration of A in the inlet gas [mol/cm^3]
c_{pb} = specific heat of the bed [cal/g·K], [J/g·K]
c_{pf} = specific heat of gas [cal/g·K], [J/g·K]
c_{ps} = specific heat of solid [cal/g·K], [J/g·K]
E = activation energy [J/mol·K], [cal/mol·K]
E_f = dispersion coefficient of gas phase [cm^2/s]
E_s = dispersion coefficient of solid [cm^2/s]
$-\Delta H$ = heat of reaction [cal/mol] [J/mol]
$(-\Delta H)_c$, $(-\Delta H)_{nc}$ = do. for catalytic and non-catalytic reactions, respectively [cal/mol]
$-\Delta H_i$ = heat of formation of i species from A [cal/mol]
h_w = wall heat transfer coefficient [cal/cm^2·K·s]
$k_{ex}a_{ex}$ = volumetric mass transfer coefficient between the ascending and descending emulsion [s^{-1}]
k_H = thermal diffusivity ($E_s c_{ps}\rho_s$) [cal/cm·K·s]
$k_{ob}a_b$ = volumetric mass transfer coefficient between bubble and emulsion [s^{-1}]
k_r = rate constant based on the emulsion phase [s^{-1}]
L_c = height of the settled bed [cm]
L_f = fluidizing bed height [cm]
L_t = total bed height [cm]
N_{Ar} = $L_f A_r U_f$ [—]
N'_H = $h_w a_w (L_t - L_f)/U_f \rho_f c_{pf}$ [—]
N_{Hw} = $h_w a_w L_f / U_f c_{pf} \rho_f$ [—]
N_{Pe} = $L_f U_f c_{pf} \rho_f / k_H$ [—]
Q = heat supplied [W]
Q_I, Q_{II} = dimensionless heat supplied or removed [—]
$R_c(c, T)$ = catalytic reaction rate based on the volume of the emulsion phase [mol/cm^3·s]
$R_{nc}(c, T)$ = non-catalytic reaction rate based on the reactor volume [mol/cm^3·s]
T = temperature [K]
ΔT = temperature increase [K]
T_c = cooling temperature [K]
T_{de} = temperature in the dense phase [K]
T_{di} = temperature in the dilute phase [K]
t = time [s]
U_f = superficial velocity of gas [cm/s]
U_s = superficial velocity of the circulating solid [cm/s]
Z = dimensionless height (z/L_f) [—]
Z_f = L_t/L_f [—]
z = height [cm]

Γ_i = dimensionless activation energy of the reaction (E_i/RT_{de}) [—]
ε_b = volume fraction of the bed occupied by the bubble phase [—]
ε_e = volume fraction of the bed occupied by the emulsion phase [—]
ε_{ede} = ε_e in the dense phase [—]
η_c = contact efficiency [—]
θ = dimensionless temperature (T/T_{de}) [—]
λ = U_s/U_f [—]
ν = fraction of solid directly contacting gas phase evaluated as the emulsion phase [—]
Ω = dimensionless heat of reaction ($(-\Delta H)c_A^\circ/c_{pf}\rho_f T_{de}$) [—]
ρ_b = bed density [g/cm^3]
ρ_{de} = density of the dense phase [g/cm^3]
ρ_f = density of gas phase [g/cm^3]
ρ_s = density of solid [g/cm^3]

〈Subscripts〉
A, B, C = substants
1, 2, 3 = reactions

Literature Cited

1) Baskakov, A. P., B. V. Berg, O. K. Vitt, N. F. Filipovsky, V. A. Kirakosyan, J. M. Goldobin and V. A. Maskaev: *Powder Tech.*, **8**, 273 (1973).
2) Boothroyd, R. G.: *Chem. Process Eng.*, **1969** (10), 108.
3) Bukur, D. and N. R. Amundson: *Chem. Eng. Sci.*, **30**, 1159 (1975).
4) Danziger, W. J.: *Ind. Eng. Chem. Process Des. Dev.*, **2**, 269 (1963).
5) El Nashaie, S. and J. G. Yates: *Chem. Eng. Sci.*, **28**, 515 (1973).
6) Endoh, I., T. Furusawa and H. Matsuyama: *Kagaku Kōgaku*, **41**, 232 (1977): also in "Catalysis Review", Marcel Dekker, New York, **19** (1), (1979).
7) Farber, L. and M. W. Morley: *Ind. Eng. Chem.*, **49**, 1143 (1957).
8) Froment, G. F.: "Chemical Reaction Engineering", Advan. Chem. Ser. No. 109, p. 1, American Chem. Soc., Washington, D. C. (1972).
9) Furusaki, S., T. Kikuchi and T. Miyauchi: *AIChE J.*, **22**, 354 (1976).
10) Gabor, J. D.: *Chem. Eng. Prog. Symp. Ser.*, **66**, (105), 76 (1970).
11) Kubie, J. and J. Broughton: *Int. J. Heat Mass Transfer*, **18**, 289 (1975).
12) Mickley, H. S. and D. F. Fairbanks: *AIChE J.*, **1**, 374 (1955).
13) Mickley, H. S. and C. A. Trilling: *Ind. Eng. Chem.*, **41**, 1135 (1949).
14) Miyauchi, T.: *J. Chem. Eng. Japan*, **7**, 201 (1974).
15) Miyauchi, T. and T. Kikuchi: Preprint of the Annual Meeting of the Soc. of Chem. Engrs., Japan, G305 (1977).
16) Miyauchi, T. and S. Furusaki: *AIChE J.*, **20**, 1087 (1974).
17) Riley, H. L.: *Trans. Inst. Chem. Engrs.*, **37**, 305 (1959).
18) Schmitz, R. A.: "Chem. Reaction Eng. Reviews", H. H. Hulburt ed., p. 156, Am. Chem. Soc. (1975).
19) Selzer, V. W. and W. J. Thomson: *AIChE Symp. Ser.*, **73**, (161), 29 (1977).
20) Shirai, T.: *Kagaku Kōgaku*, **26**, 637 (1962).
21) Shirai, T., H. Yoshitome, Y. Shoji, S. Tanaka, K. Hojo and S. Yoshida: *Kagaku Kōgaku*, **29**, 880 (1965).
22) Takahashi, M.: B. S. Thesis, Univ. of Tokyo (1975).
23) Wender, L. and G. T. Cooper: *AIChE J.*, **4**, 15 (1958).
24) Yamaguchi, R.: *Kemikaru Enjiniaringu* (in Japanese), **1967** (10), 46.
25) Yates, J. G. and P. N. Rowe: *Trans. Instn. Chem. Engrs.*, **55**, 137 (1977).
26) Yoshida, K., D. Kunii and O. Levenspiel: *Int. J. Heat Mass Transfer*, **12**, 529 (1969).
27) van Heerden, C.: *Chem. Eng. Sci.*, **8**, 133 (1958).

(Presented in part at the 42nd Annual Meeting of The Soc. of Chem. Engrs., Japan at Hiroshima, April 3, 1977.)